

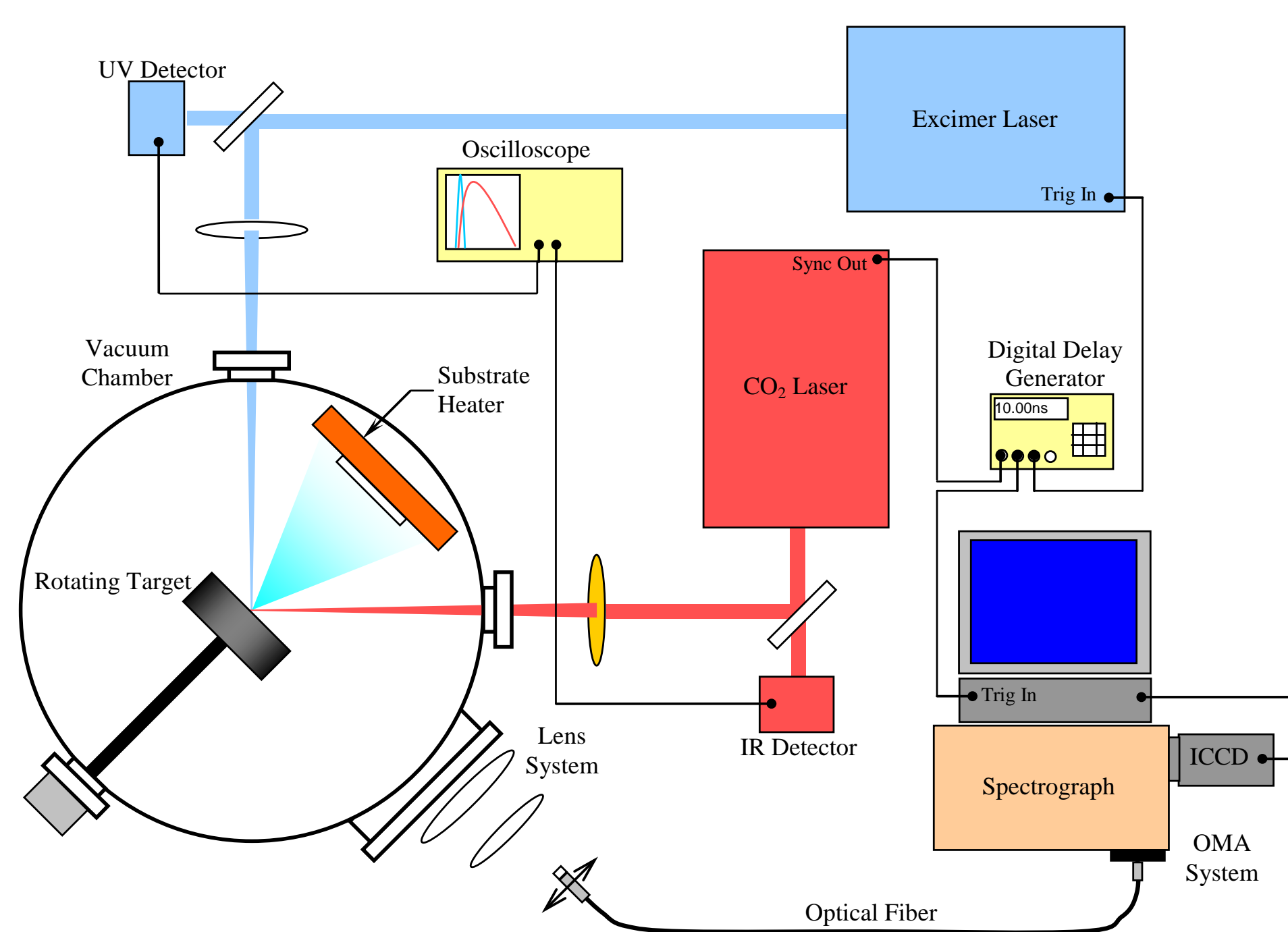
# Growth of $Ba_8Ga_{16}Ge_{30}$ Films by Pulsed Laser Ablation and Study of Growth Dynamics by Optical Emission Spectroscopy

Robert Hyde, Prithish Mukherjee, Matt Beekman, George Nolas and Sarath Witanachchi (a)

Department of Physics, University of South Florida, Tampa, FL 33620 (a) E-mail: switanac@cas.usf.edu

## Abstract

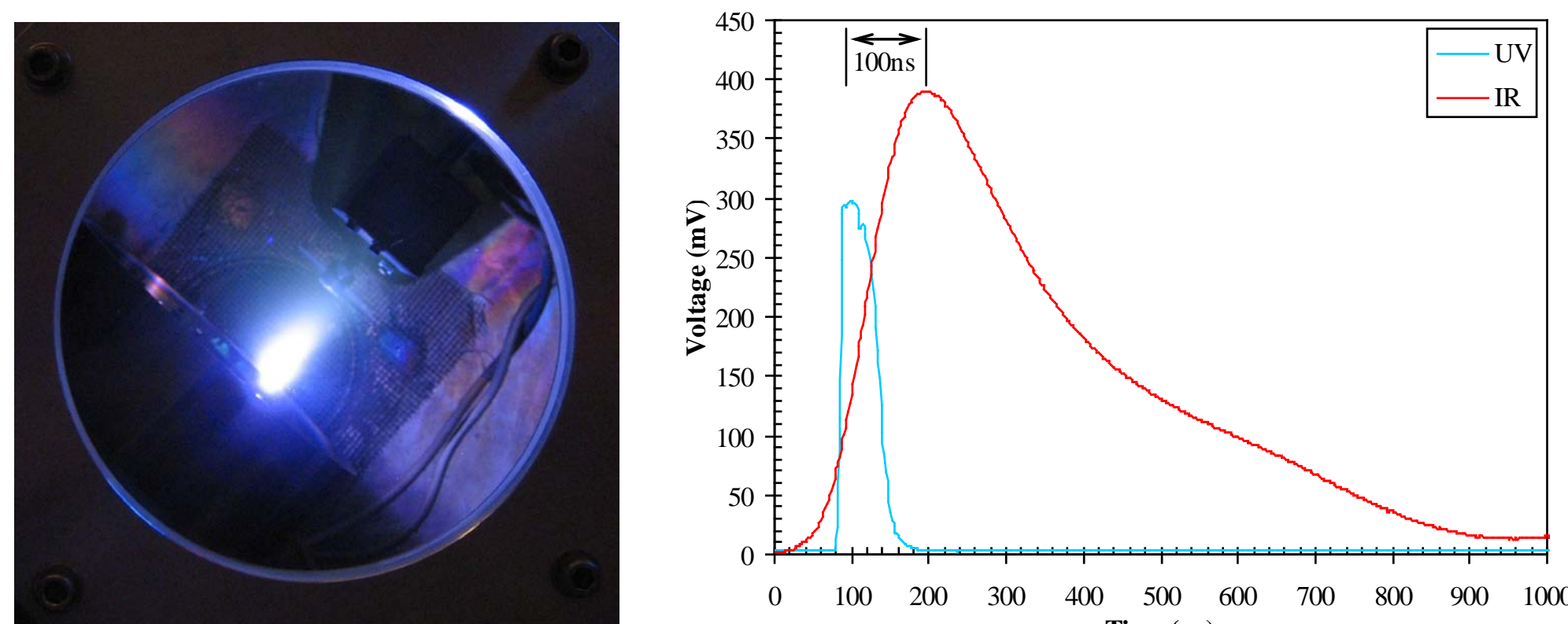
The type I clathrate  $Ba_8Ga_{16}Ge_{30}$  is a promising material for thermoelectric applications due to its very low thermal conductivity resulting from high phonon scattering by the vibrating Ba atoms in the clathrate structure. We have used a dual-laser ablation process to deposit stoichiometric films of  $Ba_8Ga_{16}Ge_{30}$ . In dual-laser ablation, excimer and  $CO_2$  laser pulses are synchronized to enhance the initial plasma temperature to facilitate the growth of poly-crystalline films with low defect densities. The crystallinity, morphology, and the stoichiometry of the films were seen to depend on the fluence of the excimer laser pulses. While low defect densities are obtained for laser fluences that are just above the ablation threshold of a  $Ba_8Ga_{16}Ge_{30}$  composite target ( $\sim 0.6 J/cm^2$ ), single laser ablation was not stoichiometric until the laser fluence reached above  $1 J/cm^2$ . In contrast, under optimum growth conditions dual-laser ablation was stoichiometric for laser fluences just above the threshold. The time-of-flight and species-resolved optical emission spectroscopy investigation of plasma expansion dynamics showed that the expansion profiles of Ba, Ga, and Ge at low fluences overlapped only in dual-laser ablation, which is required for stoichiometric film growth. Results comparing the optical emission spectroscopy, morphology, and crystalline properties of  $Ba_8Ga_{16}Ge_{30}$  films grown by the single and dual-laser processes are presented.



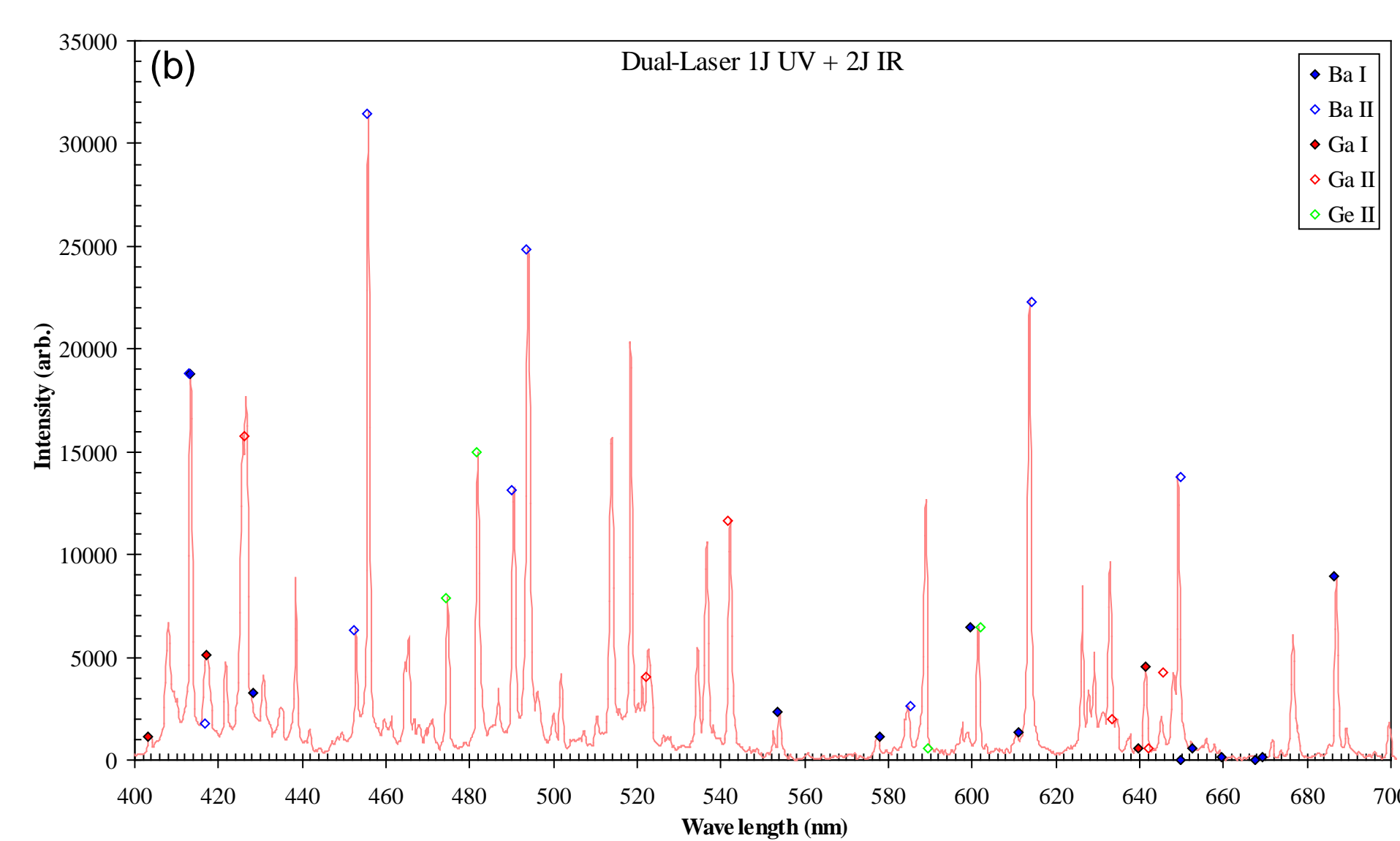
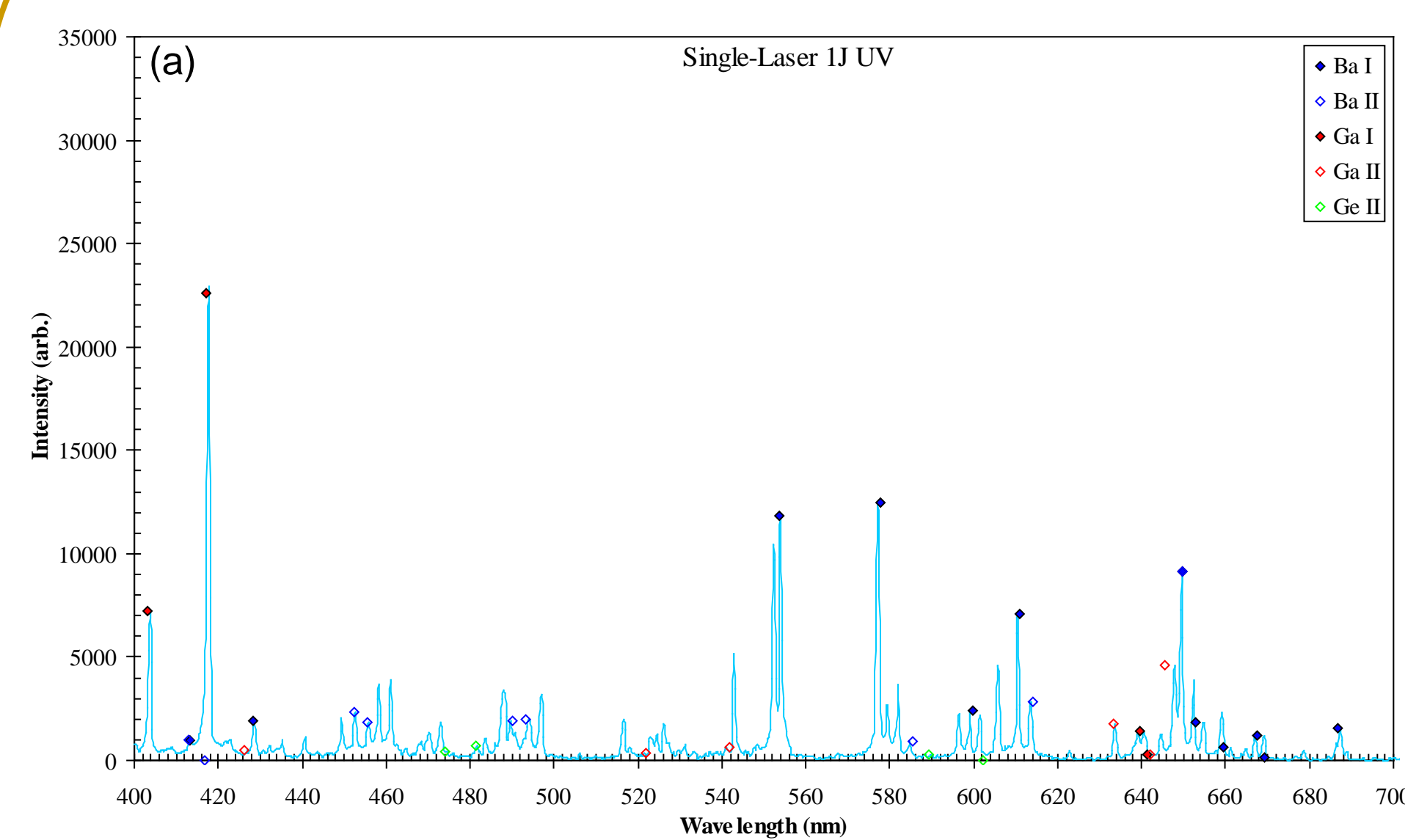
The pulsed dual-laser deposition system with the optical emission spectroscopy (OES) system. The UV laser is a KrF 248nm excimer laser and the IR laser is a  $CO_2$  10.6 $\mu m$  laser. The dual pulse synchronization is monitored on a 2 GS/s oscilloscope and controlled with a digital delay generator. OES system is triggered by the digital delay generator. Typical depositions are conducted with a vacuum pressure of  $1 \times 10^{-6}$  Torr. The target is a  $Ba_8Ga_{16}Ge_{30}$  cold-pressed target.



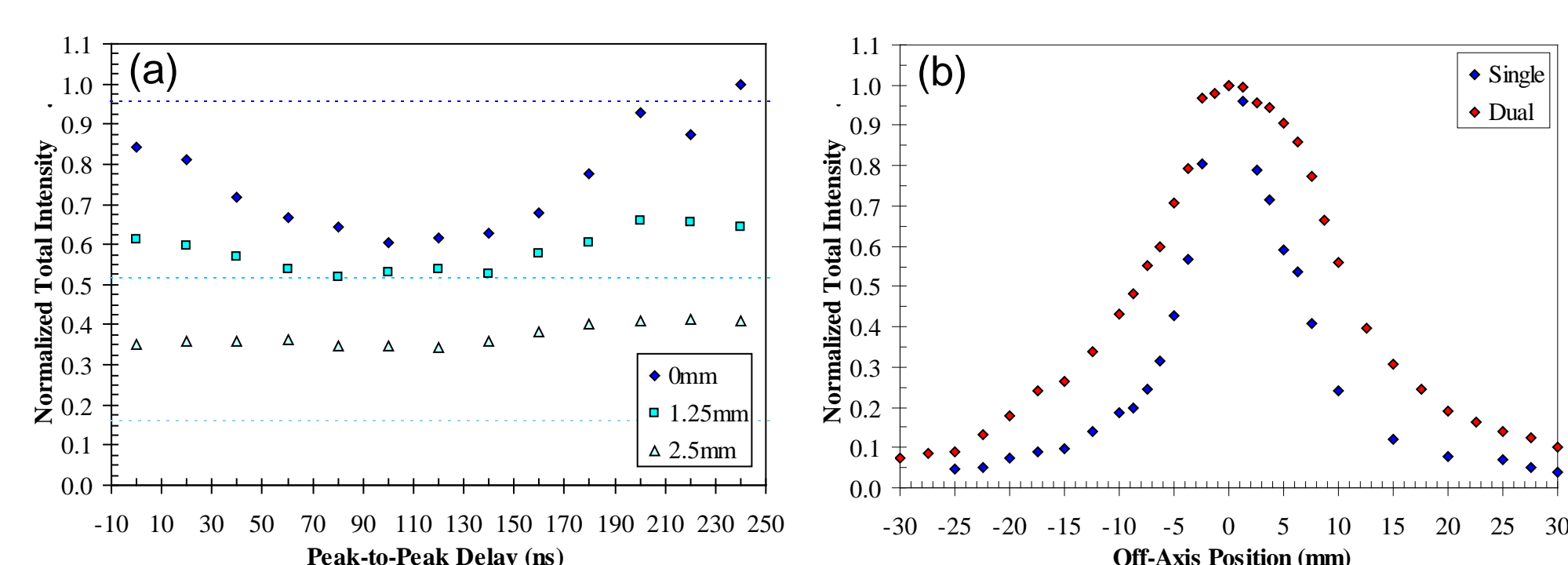
A photo of the plume generated by the pulsed laser ablation process is shown below.



The time-resolved oscilloscope traces of the excimer and  $CO_2$  laser pulses from the UV and IR detectors are shown above. A typical 100 ns peak-to-peak delay is shown.

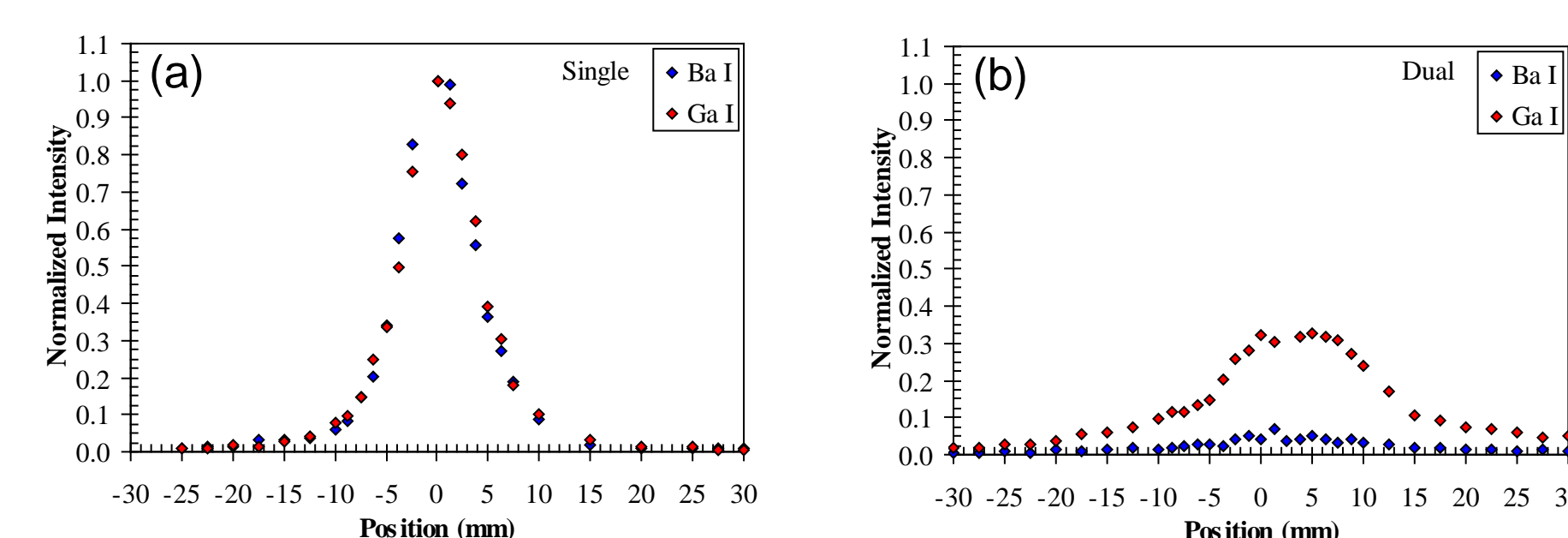


The non-gated OES visible spectrums with the neutral (I) and singly (II) ionized elements identified for barium, gallium, and germanium. Spectrums (a) for a single-laser fluence of  $1 J/cm^2$  and for (b) the dual-laser with  $1 J/cm^2$  excimer laser fluence and the  $2 J/cm^2$   $CO_2$  laser fluence. The dual-laser spectrum shows the increased intensity of the ionized elements.

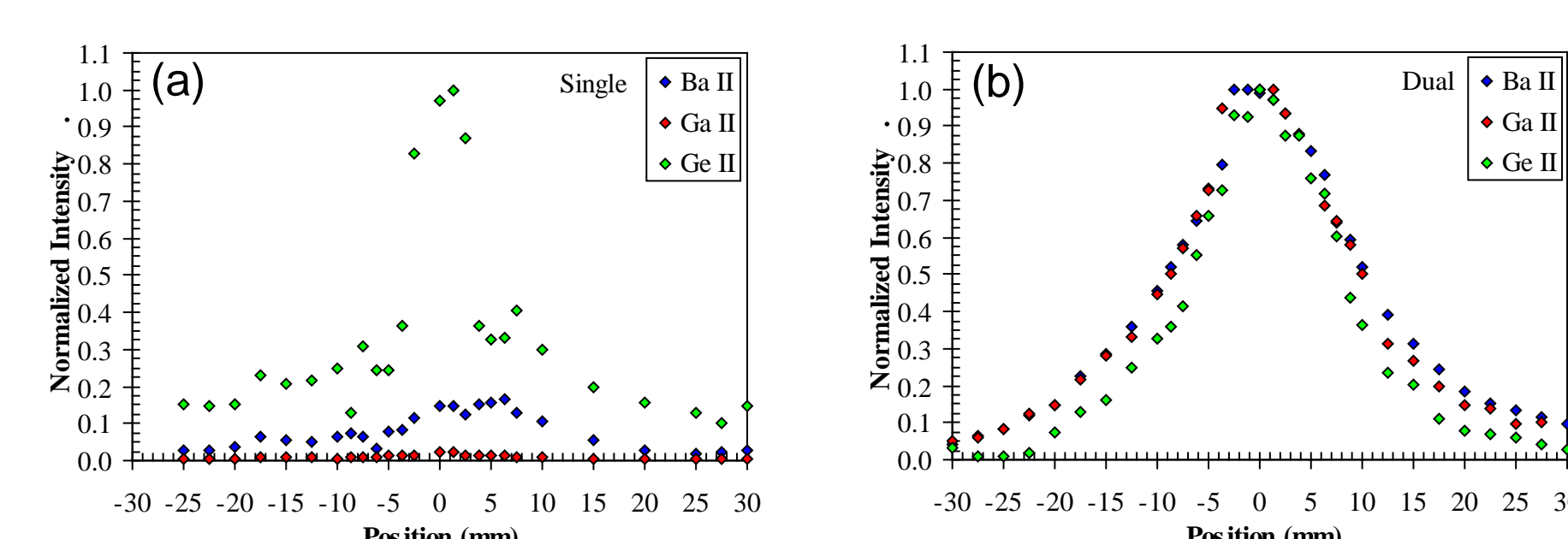


Normalized total intensity for 400 to 715 nm wavelengths, for dual-laser peak-to-peak delays with  $1 J/cm^2$  UV and  $2 J/cm^2$  IR laser fluences.

- (a) Spectrum intensities were acquired in a plane 6 mm from the target and at off-axis positions of 0 mm, 1.25 mm, and 2.5 mm. The minimum intensity at 100 ns peak-to-peak delay corresponds to broader plume expansion and higher energy coupling as compared to the single-laser intensity and expansion (dotted lines).
- (b) The total intensity cross-section where the FWHM of the single laser  $1 J/cm^2$  plume is 11.0 mm while the dual-laser plume is 19.4 mm demonstrating the broader and more energetic expansion.



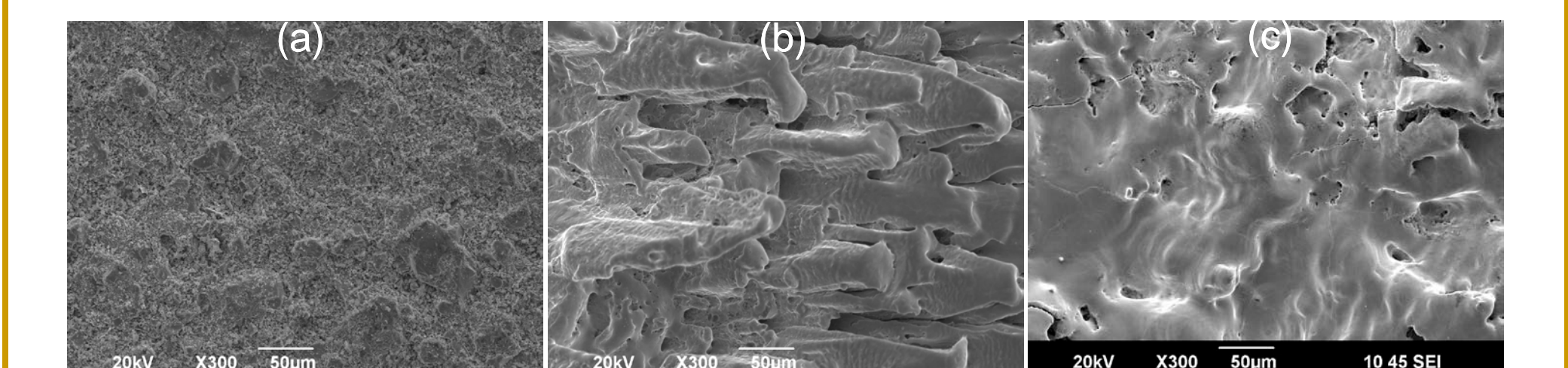
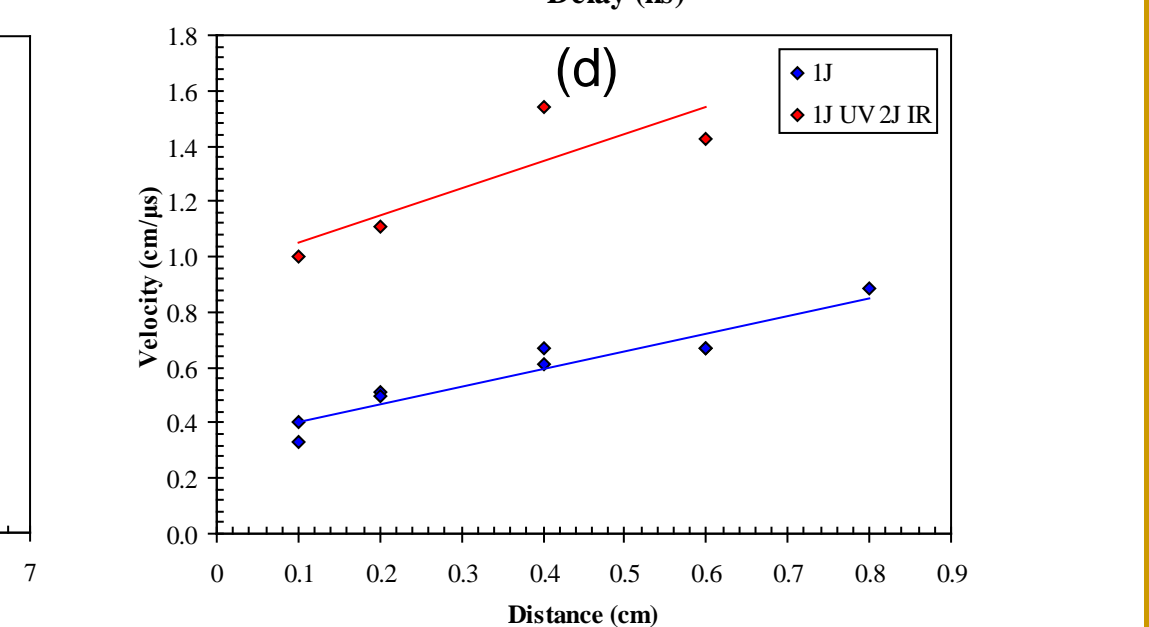
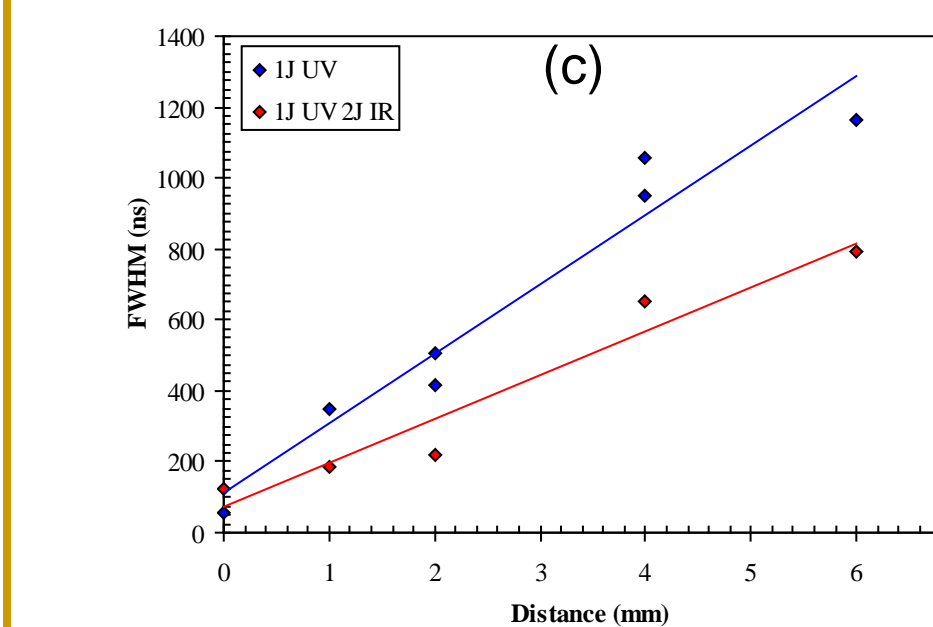
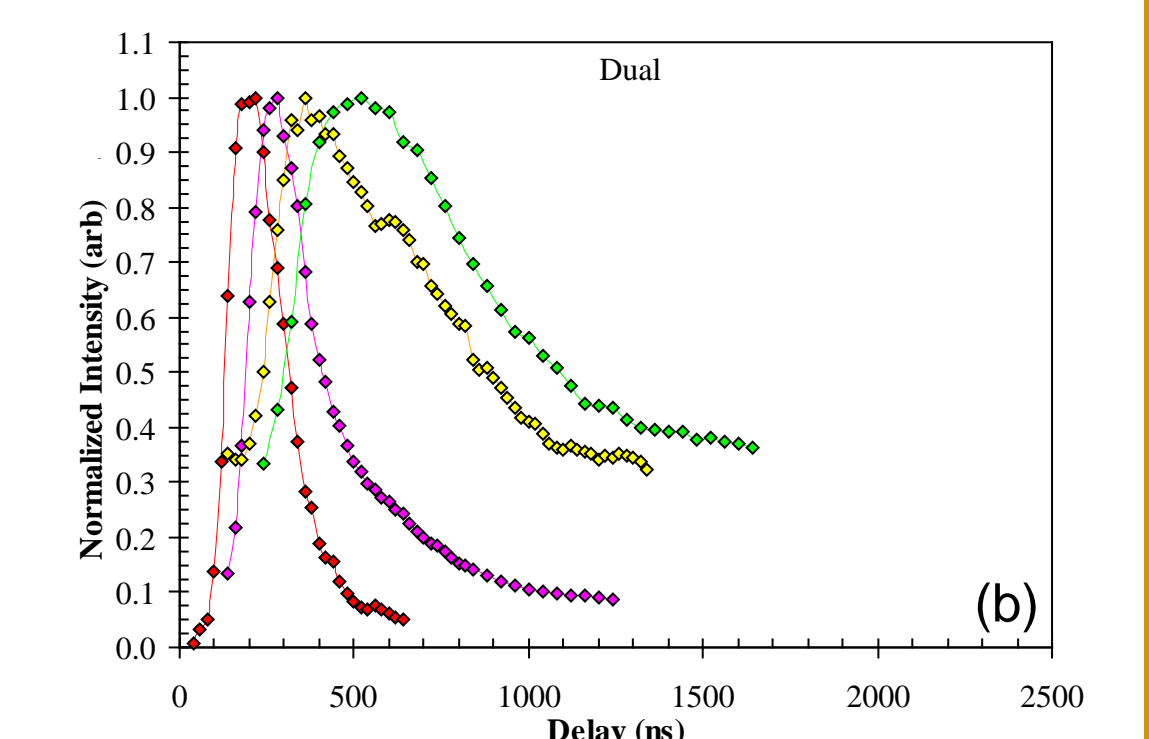
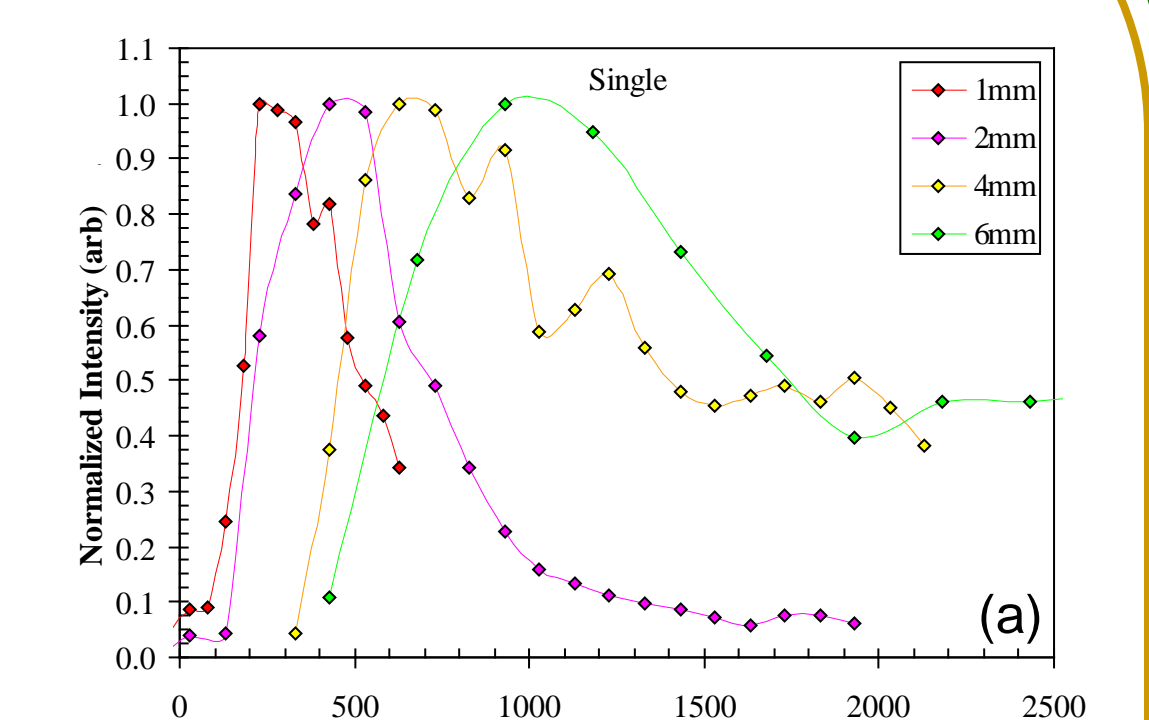
Species-resolved cross-sectional expansion profiles of neutral Ba and Ga atoms from emission spectroscopy for the (a) single-laser and (b) dual-laser plumes. Measurements were taken 2 cm from the target. The neutral emission lines of Ba I 577.76 nm and Ga I 417.20 nm are shown. Germanium does not have a neutral line in the observable range. The FWHM for the Ba and Ga lines are 8.3 mm and 8.2 mm for the single-laser, and 22.8 mm 17.3 mm for the dual-laser profiles, respectively.



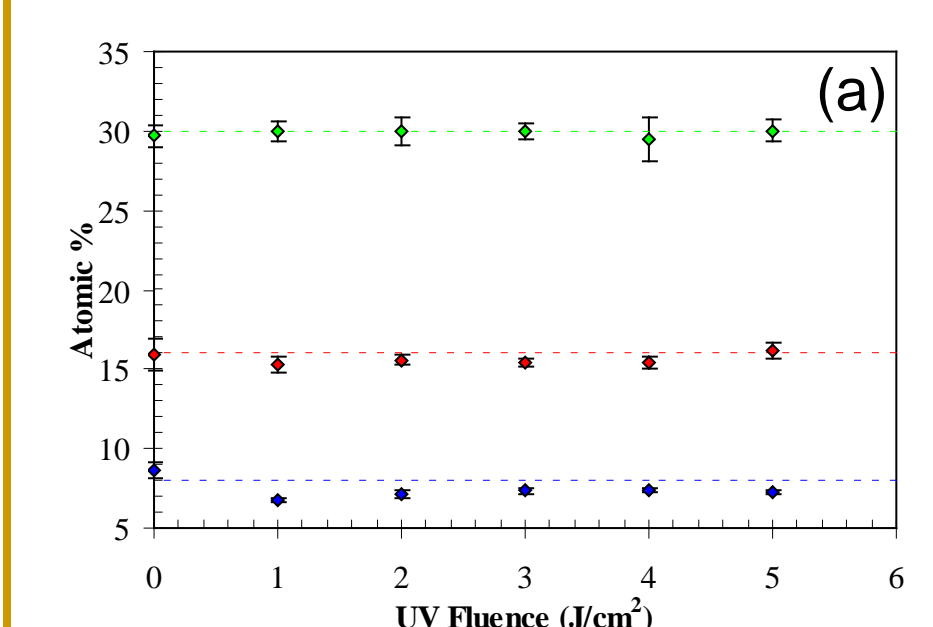
Species-resolved expansion profiles of singly ionized Ba, Ga, and Ge atoms from emission spectroscopy for (a) single-laser and (b) dual-laser plumes. The singly ionized (II) emission lines of Ba II 455.4 nm, Ga II 426.2 nm, and Ge II 481.5 nm are shown. The FWHM for the Ba, Ga, and Ge lines are 21.4 mm, 22.0 mm, and 13 mm for the single-laser, and 19.5 mm, 18.8 mm, and 15.0 mm for the dual-laser profiles, respectively.

Temporal profiles from the time-of-flight (TOF) signals for (a) single-laser and (b) dual-laser plumes at various distances from the target. The single-laser fluence was  $1 J/cm^2$  and the dual-laser fluence was  $1 J/cm^2$  UV and  $2 J/cm^2$  IR.

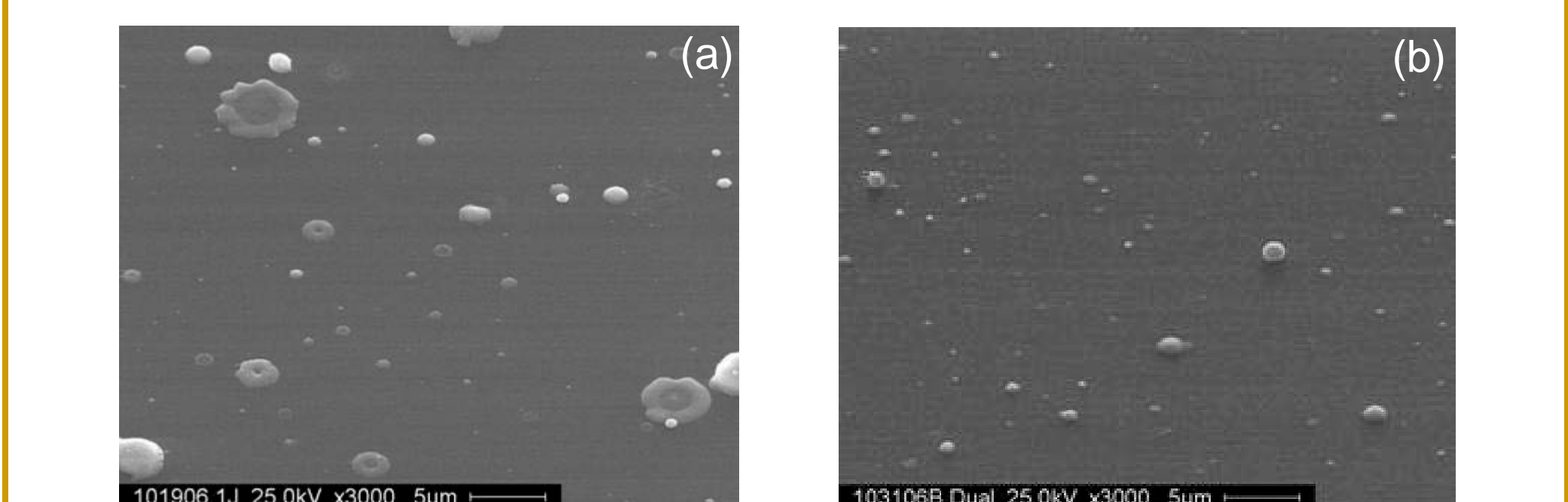
(c) The FWHM of the TOF signals indicating the temporal profile of the plasma and (d) peak plasma velocity, for the single and dual-laser generated plasma plumes at various distances from the target. Dual-laser ablated species undergo a high initial acceleration and reach much higher velocities (kinetic energy).



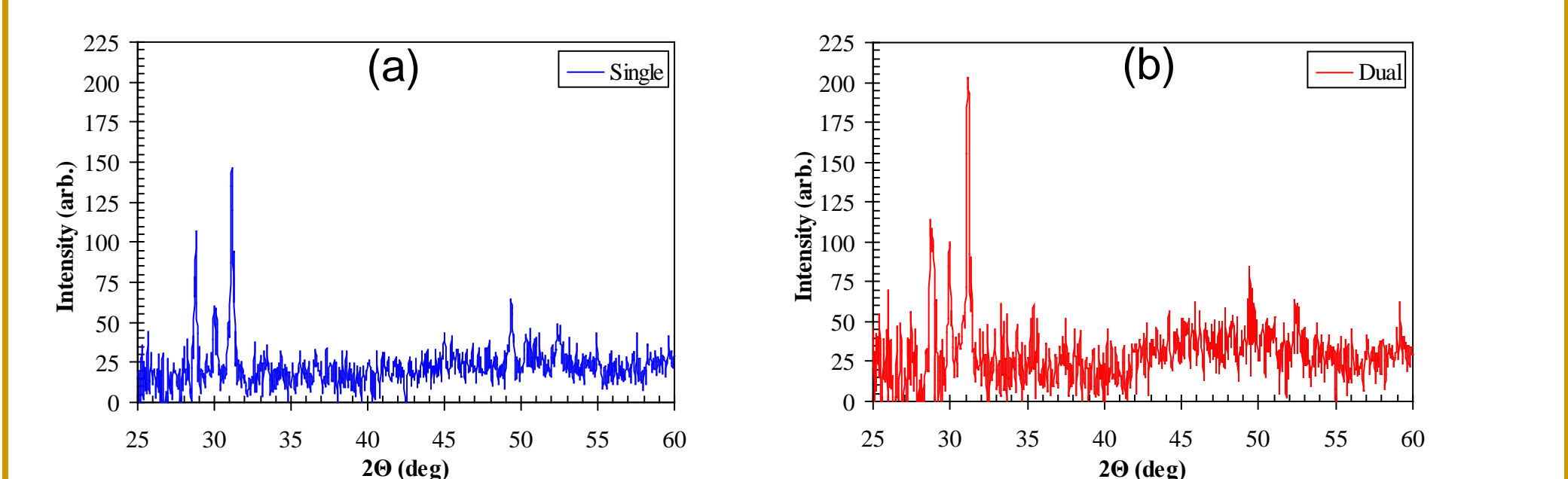
SEM of (a) the bare target and laser-target interaction sites after 1000 laser pulses of (b) single laser ablation at  $1 J/cm^2$  and (c) dual laser ablation with an excimer UV laser fluence of  $1 J/cm^2$  and  $CO_2$  IR laser fluences of  $2 J/cm^2$ . The dual-laser ablation results in a more complete melt zone at the laser-target interaction site.



Laser-target interaction site composition dependence on (a) single-laser UV and (b) dual-laser IR fluences (with  $1 J/cm^2$  UV), after 100 pulses. Near-stoichiometric removal of material is maintained.



SEM images of (a)  $1 J/cm^2$  single-laser and (b)  $1 J/cm^2$  UV with  $2 J/cm^2$  IR dual-laser with a 100 ns peak to peak delay. The large macro droplets have been eliminated from the dual-laser film.



XRD of  $Ba_8Ga_{16}Ge_{30}$  films deposited on quartz for (a) single-laser and (b) dual-laser ablations. Note the greater peak intensities for the dual-laser deposited film.

## CONCLUSIONS:

We have grown stoichiometric  $Ba_8Ga_{16}Ge_{30}$  films by the laser ablation process. Physical properties of the target favor the ejection of micron and submicron size particulates leading to poor film morphologies. We have used a dual-laser ablation process to eliminate the formation of large particulates. Dynamics of the laser ablated plasma plume has been investigated by optical emission spectroscopy. The dual-laser process produces high density of ions in comparison to the single laser process, and the expansion profiles of each species overlap, which is essential for reproducing the target stoichiometry at the substrate. Species velocities are also much higher. All these factors positively contribute to the formation of highly crystalline films of  $Ba_8Ga_{16}Ge_{30}$ .